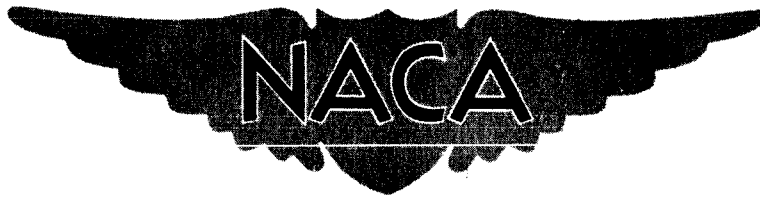




Copy 476
RM L58C21

NACA RM L58C21



1781

RESEARCH MEMORANDUM

A FEASIBILITY STUDY OF THE FLARE-CYLINDER CONFIGURATION

AS A REENTRY BODY SHAPE FOR AN INTERMEDIATE
RANGE BALLISTIC MISSILE

By James R. Hall and Benjamine J. Garland

Langley Aeronautical Laboratory
Langley Field, Va.

Declassified by authority of NASA
Classification Change Notices No. 7-44
Dated ** 9-15-84

~~DECLASSIFIED - EFFECTIVE 1-15-64~~
Authority: Memo Geo. Drobka NASA HQ.
Code ATSS-A Dtd. 3-12-64 Subj: Change
in Security Classification Marking.



NATIONAL ADVISORY COMMITTEE FOR AERONAUTICS

WASHINGTON N65-87881

May 28, 1958

FACILITY FORM 602

(ACCESSION NUMBER)

(PAGES)

(NASA CR OR TMX OR AD NUMBER)

(THRU)

(CODE)

(CATEGORY)



REF ID: A60000



NATIONAL ADVISORY COMMITTEE FOR AERONAUTICS

RESEARCH MEMORANDUM

A FEASIBILITY STUDY OF THE FLARE-CYLINDER CONFIGURATION
AS A REENTRY BODY SHAPE FOR AN INTERMEDIATE
RANGE BALLISTIC MISSILE

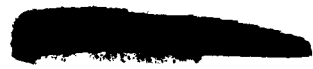
By James R. Hall and Benjamine J. Garland

SUMMARY

A study has been made of a flare-cylinder configuration to investigate its feasibility as a reentry body of an intermediate range ballistic missile. Factors considered were heating, weight, stability, and impact velocity. A series of trajectories covering the possible range of weight-drag ratios were computed for simple truncated nose shapes of varying pointedness, and hence varying weight-drag ratios. Four trajectories were chosen for detailed temperature computation from among those trajectories estimated to be possible. Temperature calculations were made for both "conventional" (for example, copper, Inconel, and stainless steel) and "unconventional" (for example, beryllium and graphite) materials. Results of the computations showed that an impact Mach number of 0.5 was readily obtainable for a body constructed from conventional materials. A substantial increase in subsonic impact velocity above a Mach number of 0.5 was possible without exceeding material temperature limits. A weight saving of up to 134 pounds out of 822 was possible with unconventional materials. This saving represents 78 percent of the structural weight. Supersonic impact would require construction of the body from unconventional materials but appeared to be well within the range of attainability.

INTRODUCTION

In the design of a ballistic-missile system, efficiency of design in the reentry body is particularly important because of the weight multiplication experienced by successive stages of the system. For a two-stage ballistic missile of 1,500-mile range, the multiplication factor is typically about 35; that is, for each 100 pounds of reentry body weight, the overall initial weight of the system is 3,500 pounds.



DECLASSIFIED - EFFECTIVE 1-15-64
Authority: Memo Geo. Drebnka NASA HQ.
Code ATSS-A Dtd. 3-12-64 Subj: Chang
in Security Classification Marking

Hence, for efficient design, it is essential that the reentry body be as light as possible. In a reentry body, the warhead constitutes the payload which must be housed in a suitable structure and made stable throughout the reentry trajectory. With a fixed payload, the only possibility of weight reduction lies in reduced structural or stabilizer weight. Structural weight is to a large extent governed by the necessity to protect the warhead from aerodynamic heating. Aerodynamic heating can be controlled in various ways - such as by providing a skin of sufficient heat capacity to limit the temperature rise to permissible material limits, by employing configurations which have low heat-transfer coefficients, and by reducing the heating potential of the reentry trajectory. It has been shown in reference 1 that blunt faces have favorable heat-transfer characteristics and that the high drag of the blunt face produces a lower velocity of reentry and hence a lower heating potential than a hemisphere nose shape.

Stability of the reentry body is required as it reenters the atmosphere in order that it fly a repeatable trajectory with its heat-sink face forward. The degree of stability required as evidenced by the magnitude of the reentry-body oscillation is undefined. It can be provided naturally by the inherent stability of the reentry body or artificially with an automatic stabilization device. The requirement is made more stringent since the range of Mach numbers extends from hypersonic to subsonic and because light weight is required.

Another requirement is low dispersion. A major source of dispersion is unknown wind conditions at the target and the amount of dispersion depends upon the length of time that the reentering body spends in the lower atmosphere. Dispersion has been found to be a function of the impact Mach number, which is a function of the ratio of weight to drag.

Ideally then, the missile should be as light as possible compatible with adequate protection from aerodynamic heating. It should have a high impact Mach number in order to reduce dispersion. It must be dynamically and statically stable. All these requirements must be met with a minimum sacrifice of simplicity.

Experience with the development of high-speed research missiles has indicated that minimum-weight configurations were flare-stabilized cylinders, the cylinder being the minimum diameter allowed by the largest component. It is believed that this same reasoning would apply to a 1,500-mile ballistic missile. The major question is whether the face or nose of the body with a relatively small diameter could tolerate the heat loads. The flat face with its low heating rates made this appear possible. The flare-cylinder configuration therefore offers a minimum size package of relatively light weight. A survey of available



information (for example, see refs. 2 to 5) on the stability of flare-stabilized bodies was made and although the information was sparse, it indicated that flare stabilization was possible throughout its reentry. The basic flare-cylinder configuration can be readily modified to reduce dispersion by reducing the nose diameter, thereby reducing the drag and increasing the impact Mach number; but, inasmuch as reduction of the nose diameter increases the heating, a compromise must be struck between impact Mach number and heating.

In order to investigate the feasibility of such a configuration, calculations have been made of the heating experienced during the reentry of a 1,500-mile-range ballistic missile. Impact Mach numbers from 0.5 to 1.89, achieved by varying the weight-drag ratio, were considered. "Conventional" (copper, Inconel, and stainless steel) materials and "unconventional" (beryllium and graphite) materials were assumed in the study. The results of the study and the conclusions drawn from it are herein presented to demonstrate the feasibility of the flare-cylinder configuration for intermediate range reentry bodies.

SYMBOLS

C_D	drag coefficient, D/qS
c_f	local skin-friction coefficient
C_p	pressure coefficient, $(p_v - p_\infty)/q$
c_p	specific heat of air at constant pressure, Btu/slug- $^{\circ}R$
c_w	specific heat of wall material, Btu/lb- $^{\circ}R$
D	drag, lb
h	heat-transfer coefficient, Btu/ft 2 - $^{\circ}R$ -sec
k	conductivity of wall material, Btu/sec-ft- $^{\circ}R$
M	Mach number
N_{St}	Stanton number, $h/(c_p \rho V)$
q	dynamic pressure, lb/sq ft





4

R_θ	Reynolds number based on momentum thickness
R	large radius of frustum, in.
r	small radius of frustum, in.
S	reference area, sq ft
T	temperature, $^{\circ}R$
t	time, sec
V	velocity, ft/sec
ρ	density of air, slug/cu ft
ρ_w	density of wall material, lb/ft ³
τ	wall thickness, ft

Subscripts:

e	edge of face
o	stagnation point
v	conditions just outside the boundary layer
w	wall
aw	adiabatic wall
∞	conditions in the undisturbed flow

DESIGN CONSIDERATIONS

Materials

It would be desirable to use conventional materials exclusively in the reentry body since their known properties simplify design and construction. Such materials as copper, Inconel, and stainless steel have proved to be effective for high-temperature applications in the hypersonic flight models investigated by the Langley Pilotless Aircraft Research Division. They have well-known properties and can surely be considered



conventional materials. Other materials are also available which have very desirable thermodynamic properties. The thermodynamic and physical properties of some conventional and unconventional materials are briefly summarized in the following table:

Material	Density, lb/cu ft	Specific heat, Btu/lb-°R	Tensile strength, lb/sq in., at -		Melting temperature, °R	Conductivity, Btu/ft-sec-°F
			100° F	1,200° F		
Conventional						
Copper	560	0.09 to 0.11	34,000	4,000	2,350	0.06 to 0.05
Inconel	520	0.11 to 0.16	84,000	56,000	2,960	0.0024 to 0.0045
Stainless steel	519	0.12 to 0.16	73,000	42,000	2,950	0.002 to 0.005
Unconventional						
Graphite ^a	---	(See fig. 1(a).)	≈1,000	-----	^b 6,900	(See fig. 1(b).)
Beryllium ^a	---	(See fig. 1(a).)	125,000	31,000	2,800	0.025 to 0.015

^aData from reference 6.

^bSublimes.

It can be seen that the three conventional metals have about the same weight density and specific heat. They are relatively heavy. Copper has low strength, especially at elevated temperatures. The melting temperature of copper is relatively low in comparison with that of Inconel and stainless steel although its conductivity is high. Copper is suitable for use at moderate temperatures under high heating rates where the capacity of the entire skin thickness is more effectively utilized because of its high conductivity. Inconel and stainless steel, although both retain their strength to higher temperatures, cannot be used in thick sections because of their low conductivity.

The property of beryllium which makes it outstanding is its very high heat capacity. It can absorb about five times as much heat as an equivalent weight of copper, for instance. It is very light and strong. The advantage of graphite is its ability to withstand very high temperatures. It does not melt but sublimes at about 6,900° R, absorbing the heat of vaporization. Graphite is light and relatively weak. Admittedly, considerable development is required in order to realize the advantages of these materials, but the reward is potentially great. Certain ceramics and metallic oxides also appear to be suitable for high-temperature use, but are considered to be in an even earlier stage of development than beryllium and graphite. Graphite is suited for use on the nose of the reentry body where high temperatures are encountered and where its sublimating characteristics may be utilized for ablative cooling. Beryllium is suited for use on the afterbody where its high heat capacity per pound can be effectively employed to decrease weight and improve stability.

Preliminary estimates of the reentry body heating indicated that a subsonic impact body could be made from copper and Inconel, but that

supersonic impact would require better materials such as beryllium and graphite for survival.

Configuration, Weight, Drag

The size of the reentry body is determined by the size of the warhead which it must carry. One of the sizes suitable for preliminary estimates was given to be a cylinder 19 inches in diameter and 42.5 inches long. A flare-cylinder was designed to contain the warhead and is shown in figure 2(a). A 10° flare was chosen on the basis of its successful use on a number of hypersonic free-flight vehicles investigated by the Langley Pilotless Aircraft Research Division. The flare maximum diameter of 26 inches provides a static margin of about 1 cylinder diameter. Preliminary estimates indicated that conventional materials would suffice for this flat-nosed configuration since its impact velocity was subsonic. Based on experience and preliminary estimates, skin thicknesses were chosen as shown in figure 2(a). The weight of the components and the center of gravity are also shown. The total weight of this reentry body is 822 pounds. A possible future weight for beryllium is shown to be 688 pounds. This value represents a saving of 78 percent of the structural weight.

The total drag of the configuration is composed of flat-face pressure drag, flare pressure drag, base drag, and friction drag. In order to estimate the drag, the face-drag coefficient was assumed to be equal to 0.8 total-pressure coefficient or $0.8 \left(\frac{p_0 - p_\infty}{0.7 p_\infty M_\infty^2} \right)$. This approximation has been shown to be quite good. The flare-drag coefficient was assumed to be equal to that for a cone frustum, or $\left[1 - \left(\frac{r}{R} \right)^2 \right]$ times the value of C_p for a 10° cone, based on the flare base area. The base-drag coefficient used was the three-dimensional value from reference 7. The friction drag was not considered because it was negligible below an altitude of 100,000 feet where most of the heating occurs. Subsonic drag coefficients were obtained from unpublished measurements obtained by the Langley Pilotless Aircraft Research Division for a very similar configuration. The variation of component drag coefficients times reference area $C_{D,S}$ with Mach number is presented in figure 3(a).

The relatively low impact Mach number estimated for this configuration would produce undesirably high dispersions. In order to reduce the dispersion, it was necessary to increase the impact Mach number by increasing the ratio of weight to drag. Since minimum weight was essential, a reduction of drag was required. A convenient systematic

way to vary the drag was to employ cone frustum noses of increasing pointedness. The variation of $C_D S$ with Mach number was computed for such a family of five noses ranging from blunt to pointed and is shown in figure 3(b). A semiangle of 14.5° was chosen for the frustum rather arbitrarily because some measurements had been made on frustums of this shape. The drag coefficient of the frustum cone was obtained as described previously for the flare. The value of $C_D S$ of the noses is seen to decrease markedly as the diameter of the front face is reduced, the pointed reentry body having only one-eighth the drag of the bluff-nose body at high Mach numbers.

Trajectories

An envelope of trajectories was computed for the entire possible range of weight-drag ratios of the reentry body. Trajectories were computed on digital equipment with initial conditions of reentry from reference 8 of velocity equal to 14,800 feet per second, altitude equal to 316,000 feet, reentry angle equal to -38.7 (assuming that the reentry angle was the negative of the exit angle), and initial wall temperature equal to ambient atmospheric temperature. As expected, increasing nose pointedness increased the velocity throughout the reentering period and increased the impact Mach number. The range of impact Mach numbers varied from 0.5 for the blunt-nose configuration to 8.0 for the pointed configuration. Heating estimates indicated that it would be necessary to restrict the impact Mach number of the reentry body to under 2.0 in order to avoid impossibly severe temperatures with practical material thicknesses.

In order to evaluate the feasibility of the aforementioned configurations, four trajectories covering the range of impact Mach numbers below 2.0 were selected for detailed heating calculations. The impact Mach numbers chosen were 0.5, 1.05, 1.49, and 1.89. The trajectories are depicted in figure 4. The subsonic-impact case corresponded to the bluff-nose configuration. The three supersonic-impact cases corresponded to frustum minor diameters of 11, 10.2, and 9.2 inches. In order to simplify computations, it was decided to conduct all subsequent heating computations for a single nose diameter of 10.2 inches by using the previously computed trajectories. The error induced in the heat-transfer coefficients by this assumption is approximately 5 percent. It was felt that this was an acceptable error in view of the overall precision of the assumptions.

The nose frustum having a 10.2-inch minor diameter is shown in figure 2(b). Preliminary estimates showed that for an impact Mach number of 1.89, conventional materials could not be employed, but that

graphite and beryllium might be satisfactory. Estimated thicknesses required of the graphite nose and beryllium afterbody give the component weights tabulated below the figure, and a total weight of 835 pounds.

HEATING CALCULATIONS

Nose

The nose experiences the greatest heating rate on the reentry body. Three points were chosen at which to make detailed heating computations - the stagnation point, a point at the edge of the flat face, and a point at the rear of the nose frustum as shown in figure 2. Temperature profiles were computed for the supersonic impact trajectories at each of these points. For the subsonic impact configuration a single determination made at the edge of the face was felt to be adequate.

The variation of heat-transfer coefficient at the stagnation point was computed by using the theory of reference 9 for a hemisphere nose and halving the computed values to apply to a flat face as demonstrated in reference 10. The accuracy of the hemispherical theory was improved by using the experimental value of the stagnation-point velocity gradient instead of the theoretical value. The values of the heat-transfer coefficients thus computed are shown in figure 5 plotted against time. It should be noted that the method used assumes perfect gas conditions at all Mach numbers. The use of a real gas theory such as reference 11 would considerably reduce the heating rates at the higher Mach numbers; consequently, the calculations presented herein are very conservative.

In order to obtain the heat-transfer coefficient at the edge of the face, it was assumed that transition would occur at a Reynolds number of 250 based on momentum thickness. This assumption is somewhat conservative for a highly polished surface as shown by references 12 and 13 wherein transition was delayed up to values of R_θ of 1,200. Unpublished results from experiments conducted by the Langley Pilotless Aircraft Research Division on a flat face showed that as R_θ increased to the value of 250, the ratio of local heat-transfer coefficient to stagnation-point heat-transfer coefficient h/h_0 increased from 1.0 to 1.3, whereupon transition occurred, and the ratio h/h_0 increased more rapidly to the value 3.5 at a value of R_θ of 700. Based on these experiments, a relationship between h at the edge of the face and h at the stagnation point was devised which led to the edge heat-transfer coefficients presented in figure 5 as a function of time. An additional heat input existed at the corner because of heating from

the side. This effect was neglected because the magnitude of the effect in the case of the $M = 1.9$ trajectory increased h only about 5 percent of the maximum value of h which was small considering the gross nature of the study and the fact that other effects such as conduction were not considered. Conduction in the vicinity of the corner can have a powerful effect as shown in reference 10 wherein the measured maximum temperatures on a truncated copper nose were actually lower at the corner than at the stagnation point. (Maximum temperature occurred some time after peak Mach number.)

The values of h at the rear of the nose frustum were computed by using the conical theory of Van Driest for a turbulent boundary layer (ref. 14), the reference length being the contour length to the rear of the frustum and local conditions on the cone behind a normal shock.

Temperature profiles on the nose were calculated by using the heat-transfer coefficients shown in figure 5 at the stagnation point and corner at the front face and at the rear of the nose frustum for the supersonic impact trajectories by the method of Dusinberre (ref. 15). The method was modified by the inclusion of a radiation term which had considerable effect at the elevated temperatures encountered. Thin-wall theory was used in the determination of wall-temperature history at the corner of the copper face for the subsonic impact trajectory.

Afterbody

Heating on the afterbody is sufficiently less severe than on the nose that much thinner skins can be used, and temperature calculations are amenable to the simple thin-wall method. Two points were chosen as representative of the afterbody, namely, a point on the cylinder immediately behind the nose and a point on the flare immediately behind the cylinder-flare juncture. Only turbulent heat-transfer coefficients for these points were computed by using the theory of Van Driest (ref. 14) and the modified Reynolds analogy $N_{ST} = 0.6C_F$ from reference 16. The contour length from the stagnation point and local conditions were used. On the conical flare, being very conservative, the heat-transfer coefficient for half the Reynolds number was used. Temperature histories were computed by using the thin-wall equation

$$\Delta T = \frac{h(T_{aw} - T_w)\Delta t}{\rho_w c_w T}$$

RESULTS AND DISCUSSION

The temperatures computed for the subsonic-impact trajectory ($M = 0.5$) at the edge of the front face and on the cylinder and flare are presented in figure 6. It can be seen that the computed temperatures are well below the material limits for the $3/4$ -inch copper wall at the edge of the face and the 0.1-inch Inconel wall of the cylinder and flare. It can be concluded that the weight assumed for the subsonic impact vehicle was based on valid skin thicknesses, and that the estimated weight used in the trajectory calculation was realistic. A calculation of the temperature of a 0.1-inch-thick beryllium flare is shown in figure 6 to give a maximum temperature of $1,500^{\circ}$ R which is about 100° less than for an Inconel flare. The result could be approximated by assuming the maximum temperature to be inversely proportional to the average specific heat times density of the two metals. Applying the same relationship to the flat face of the vehicle, it can be concluded that the use of beryllium in place of copper and Inconel would be possible from the viewpoint of temperature limitations. As indicated in the section on models, the use of beryllium in place of copper and Inconel would permit a weight reduction of up to 134 pounds.

It should be noted that the computed temperatures are under $1,600^{\circ}$ R, which offers a considerable safety margin under the melting temperatures of copper and Inconel. It should therefore be possible to increase the impact Mach number beyond the value of 0.5 which was used for these computations without exceeding material limitations. Since the value $1,600^{\circ}$ R represents a conservative estimate of the working maximum temperature of beryllium, any increase in the impact Mach number would require increased thicknesses of beryllium in order not to exceed this figure, which would, of course, decrease the weight advantage accruing from the use of beryllium.

The temperatures computed for the three supersonic impact trajectories ($M = 1.05$, 1.48, and 1.89) for a graphite and beryllium body are presented in figures 7 to 10. The maximum nose temperatures are seen to occur about 30 seconds after beginning reentry. The stagnation-point maximum temperatures varied from $2,900^{\circ}$ for the $M = 1.05$ trajectory to $3,300^{\circ}$ R for the $M = 1.89$ trajectory. Corner maximum temperatures varied from $3,500^{\circ}$ R to $4,250^{\circ}$ R. Maximum temperatures at the rear of the frustum varied from $2,000^{\circ}$ R to $2,750^{\circ}$ R. The temperature differences through the skin are very high - briefly reaching a maximum temperature difference of $3,100^{\circ}$ R across the first half of the thickness for the $M = 1.89$ trajectory 28 seconds after reentering. For the $M = 1.05$ trajectory, the corresponding temperature difference is $2,400^{\circ}$ R. The computed temperatures, although high, are considerably below the sublimation temperature of graphite. Although the problem



of thermal shock is serious, it is felt that these results indicate that a nose could be developed with graphite as the principal component which would withstand the heating associated with supersonic reentry.

In order to investigate the possibility of employing a more conventional material than graphite for the nose frustum, temperature computations were made for a copper nose frustum, using an impact Mach number of 1.05. The results, presented in figure 10, show that the temperature of the stagnation point and the base of the frustum does not exceed material limitations, but that the corner of the face melts at about 29 seconds despite the doubled wall thickness (2 inches) at the corner. It must be noted that the copper is five times as dense as graphite and would impose a weight penalty of 236 pounds on the reentry body if it was used.

The temperature on the 0.5-inch beryllium cylinder and flare is seen to be below $1,550^{\circ}$ R for all trajectories. Indeed, for the $M = 1.49$ and $M = 1.05$ trajectories, the assumed thickness of 0.5-inch beryllium could be reduced considerably without exceeding safe maximum temperatures.

CONCLUDING REMARKS

In the foregoing study many simplifying approximations have been made in order to expedite the determination of the feasibility of the flare-cylinder configuration for an intermediate range missile. The approximations made were intended to give a realistic estimate of the most severe conditions which the reentry body would experience. When in doubt, conservative approximations were used. A cone frustum nose has been used throughout this study because it was amenable to simplified analysis. This is not meant to imply that other nose shapes might not be as good or superior from overall considerations such as heating, stability, weight, and strength. The temperatures computed for the hypothetical reentry body of this report indicate that such a flare-stabilized design is entirely possible with a subsonic impact nose and feasible with a supersonic impact nose.

Langley Aeronautical Laboratory,
National Advisory Committee for Aeronautics,
Langley Field, Va., March 6, 1958.




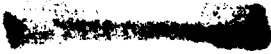


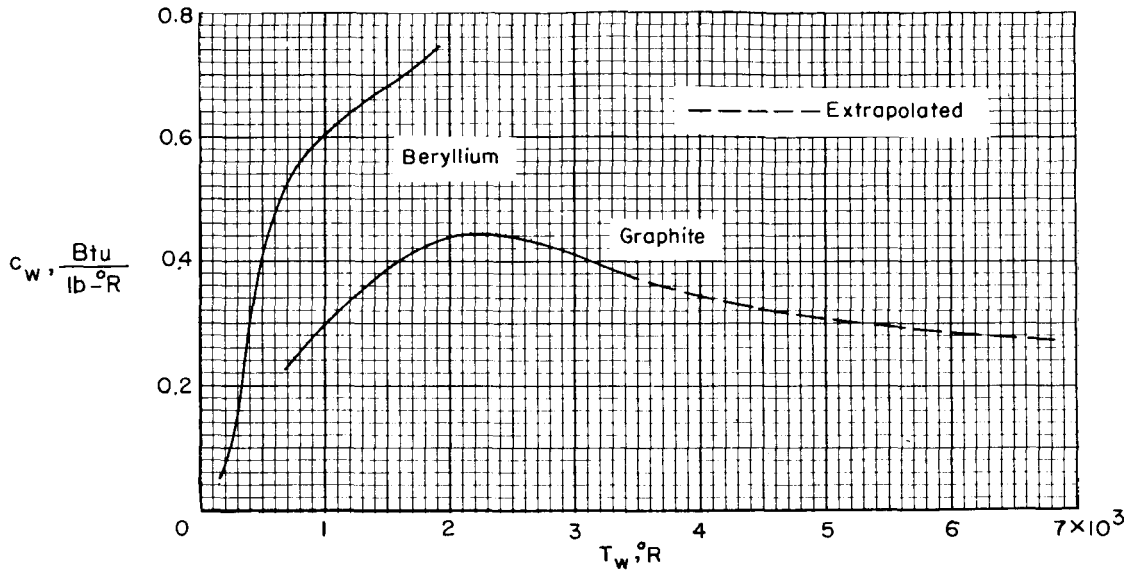
REFERENCES

1. Allen, H. Julian, and Eggers, A. J., Jr.: A Study of the Motion and Aerodynamic Heating of Missiles Entering the Earth's Atmosphere at High Supersonic Speeds. NACA TN 4047, 1957. (Supersedes NACA RM A53D28.)
2. Moeckel, W. E.: Some Effects of Bluntness on Boundary-Layer Transition and Heat Transfer at Supersonic Speeds. NACA Rep. 1312, 1957. (Supersedes NACA TN 3653.)
3. Dennis, David H., and Syvertson, Clarence A.: Effects of Boundary-Layer Separation on Normal Force and Center of Pressure of a Cone-Cylinder Model With a Large Base Flare at Mach Numbers From 3.00 to 6.28. NACA RM A55H09, 1955.
4. McFall, John C., Jr.: Dynamic Stability Investigation of Two Right Circular Cylinders in Axial Free Flight at Mach Numbers From 0.4 to 1.7. - Fineness-Ratio-2.56 Cylinder and Fineness-Ratio-4.0 Cylinder With Flared Afterbody. NACA RM L56L28, 1957.
5. Becker, John V., and Korycinski, Peter F.: Heat Transfer and Pressure Distribution at a Mach Number of 6.8 on Bodies With Conical Flares and Extensive Flow Separation. NACA RM L56F22, 1956.
6. Battelle Memorial Institute (under direction of C. R. Tipton, Jr.): Materials - General Properties. AECD-3647, The Reactor Handbook, vol. 3, sec. 1, U. S. Atomic Energy Comm., Feb. 1955.
Stacy, J. T.: Beryllium and Its Alloys. Ch. 1.4, pp. 55-94.
Slyh, J. A.: Graphite. Ch. 1.9, pp. 133-153.
7. Love, Eugene S.: Base Pressure at Supersonic Speeds on Two-Dimensional Airfoils and on Bodies of Revolution With and Without Fins Having Turbulent Boundary Layers. NACA TN 3819, 1957.
8. Harry, Charles H.: An Analysis of the Performance and Errors of Ballistic Missiles. Rep. No. DR-1769, Bur. Aero., Res. Div., Sept. 1955.
9. Sibulkin, M.: Heat Transfer Near the Forward Stagnation Point of a Body of Revolution. Jour. of Aero. Sci. (Readers' Forum), vol. 19, no. 8, Aug. 1952, pp. 570-571.
10. Stoney, William E., Jr.: Local Heat Transfer to Blunt Noses at High Supersonic Speeds. NACA RM L57D25c, 1957.

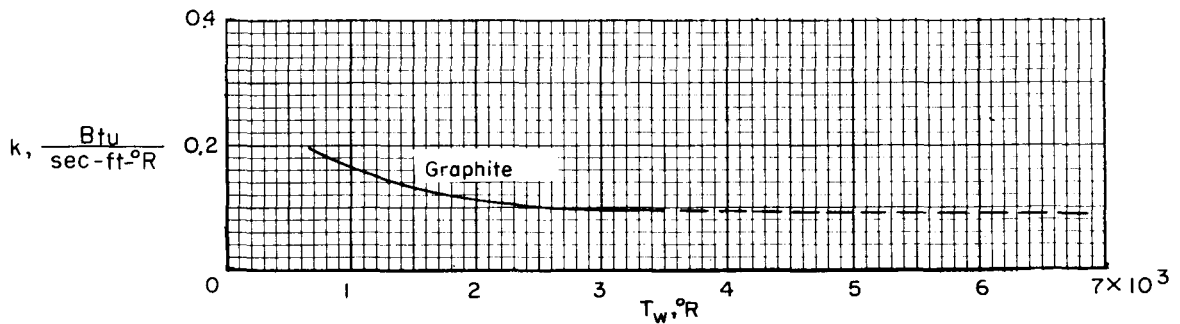




11. Fay, J. A., and Riddell, F. R.: Theory of Stagnation Point Heat Transfer in Dissociated Air. Jour. of Aero. Sci., vol. 25, no. 2, Feb. 1958, pp. 73-85, 121.
 12. Buglia, James J.: Heat Transfer and Boundary-Layer Transition on a Highly Polished Hemisphere-Cone in Free Flight of Mach Numbers Up to 3.14 and Reynolds Numbers Up to 24×10^6 . NACA RM L57D05, 1957.
 13. Hall, James R., Speegle, Katherine C., and Piland, Robert O.: Preliminary Results From a Free-Flight Investigation of Boundary-Layer Transition and Heat Transfer on a Highly Polished 8-Inch-Diameter Hemisphere Cylinder at Mach Numbers Up to 3 and Reynolds Numbers Based on a Length of 1 Foot Up to 17.7×10^6 . NACA RM L57D18c, 1957.
 14. Van Driest, E. R.: The Problem of Aeronautical Heating. Aero. Eng. Rev., vol. 15, no. 10, Oct. 1956, pp. 26-41.
 15. Dusinberre, G. M.: Numerical Methods for Transient Heat Flow. Trans. A.S.M.E., vol. 67, no. 8, Nov. 1945, pp. 703-712.
 16. Rubesin, Morris W.: A Modified Reynolds Analogy for the Compressible Turbulent Boundary Layer on a Flat Plate. NACA TN 2917, 1953.
- 
- 



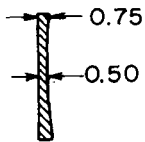
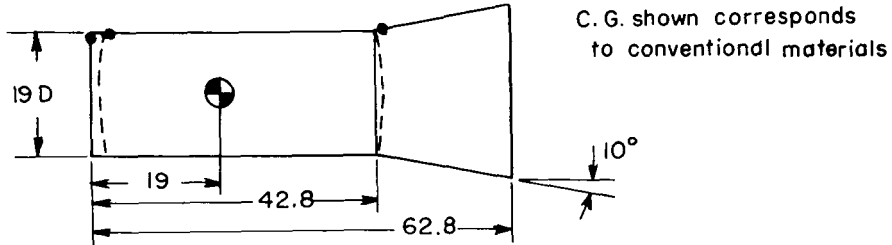
(a) Specific heat.



(b) Conductivity.

Figure 1.- Thermodynamic properties of beryllium and graphite.

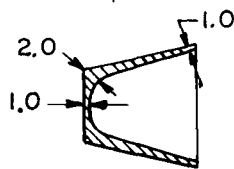
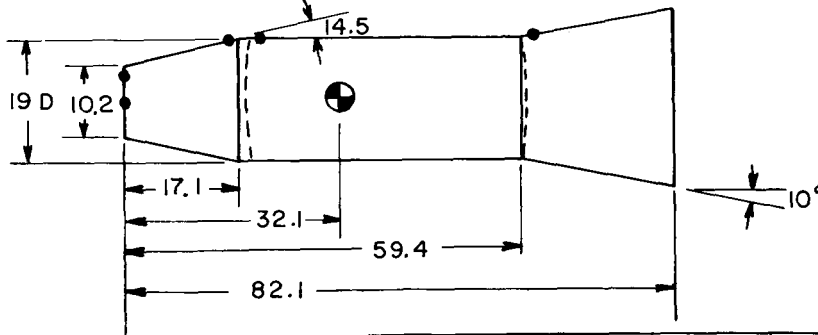
Dots indicate points employed in temperature computations.



Component	Conventional			Unconventional		
	Material	Thickness	Weight	Material	Thickness	Weight
Nose	Copper	.50-.75	55	Beryllium	.50-.75	13
Cylinder	Inconel	.10	75	Beryllium	.10	16
Flare	Inconel	.10	42	Beryllium	.10	9
Bomb	—	—	650			650
Total			822			688

(a) Subsonic impact configuration.

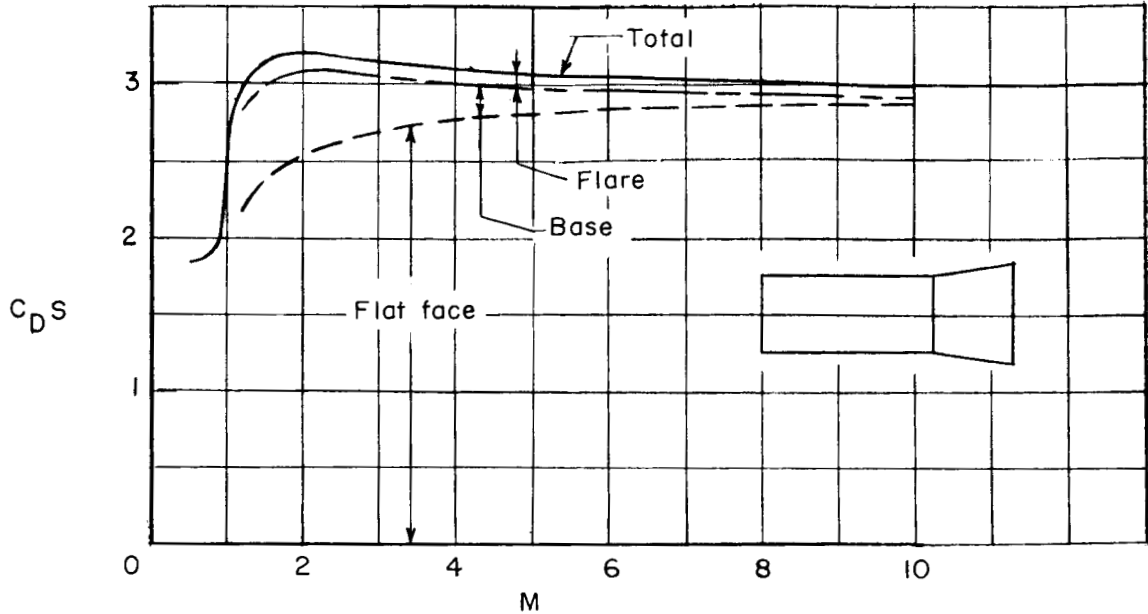
Dots indicate points employed in temperature computations.



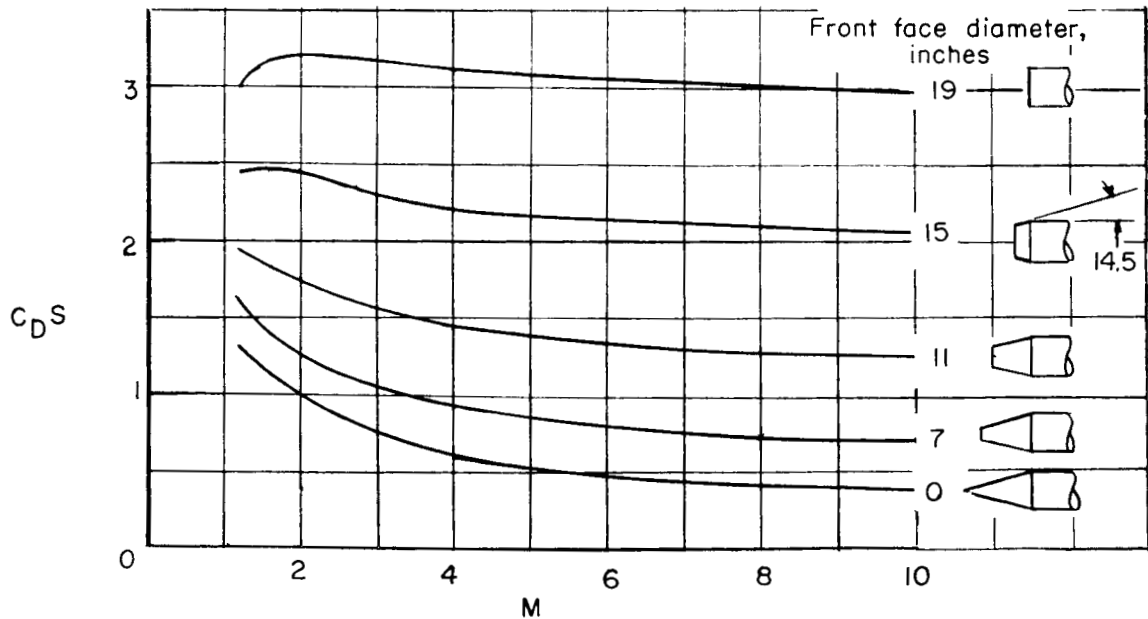
Component	Material	Thickness	Weight
Nose	Graphite	10.30	59
Cylinder	Beryllium	0.5	80
Flare	Beryllium	0.5	46
Bomb	—	—	650
Total			835

(b) Supersonic impact configuration.

Figure 2.- Reentry bodies studied in this report. All dimensions are in inches.



(a) Component $C_D S$ of bluff-nose configuration.



(b) Total $C_D S$ of configurations of different pointedness.

Figure 3.- Variation of $C_D S$ based on area of 1 sq ft with Mach number.
All dimensions are in inches.

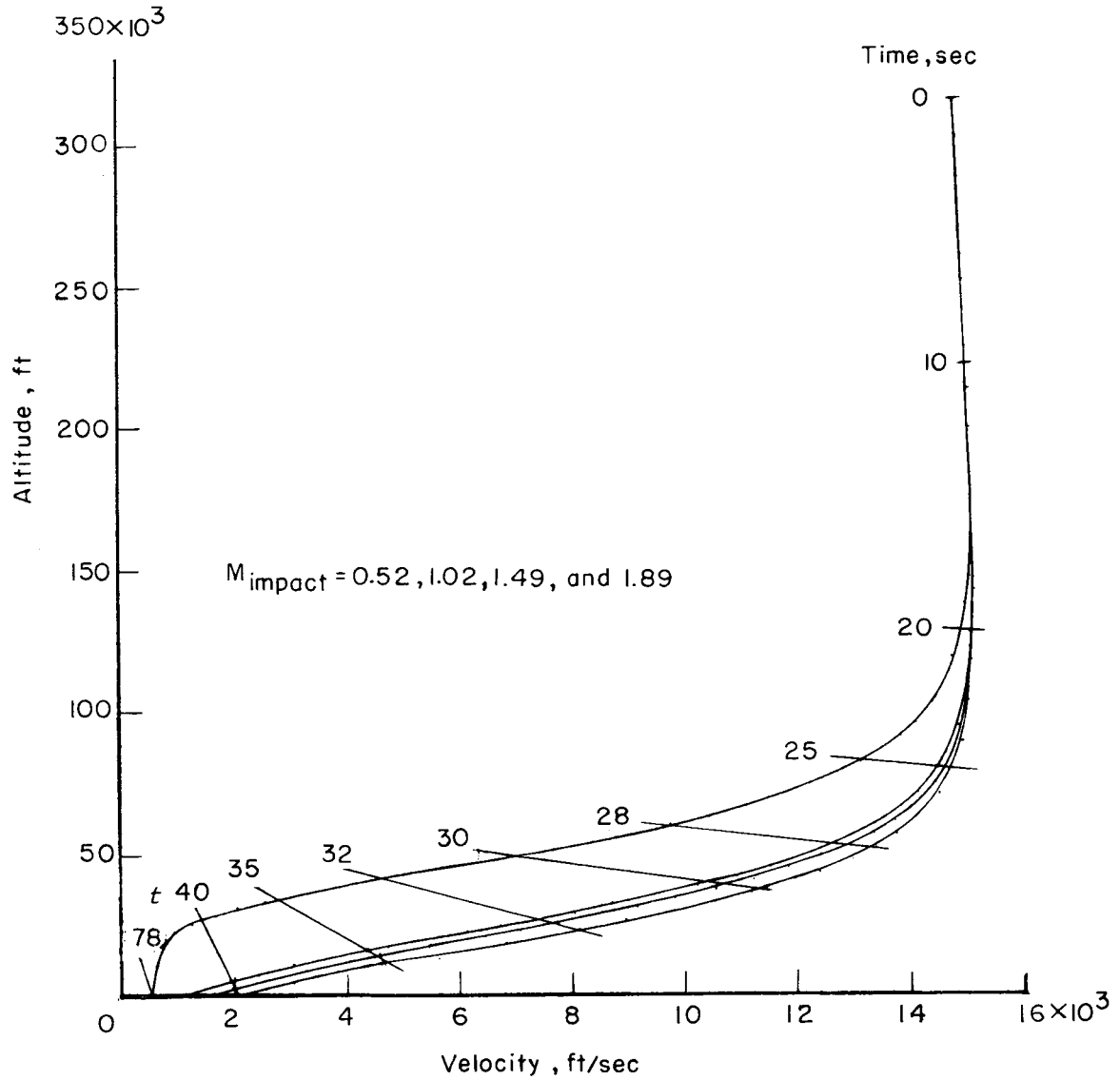


Figure 4.- Reentry trajectories considered in heating computations.

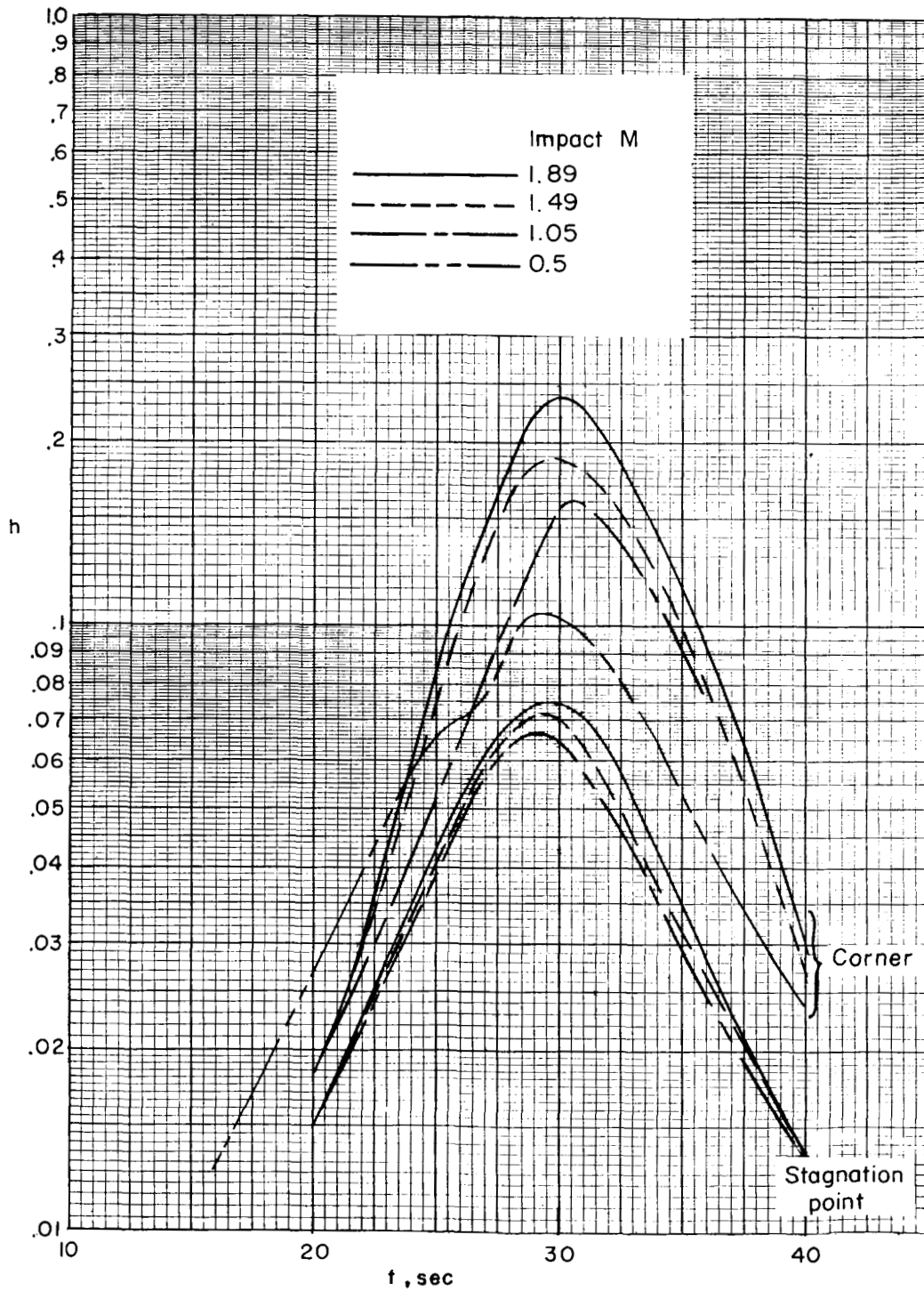


Figure 5.- Heat-transfer coefficients used in stagnation-point and corner temperature computations.

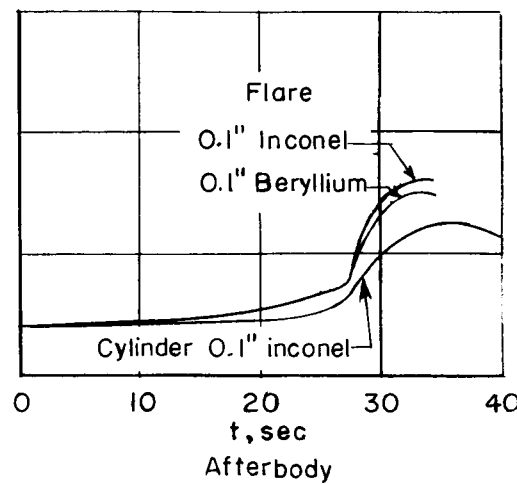
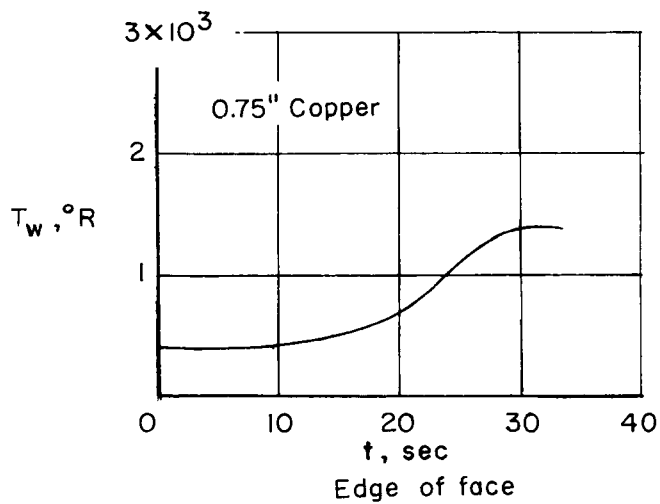
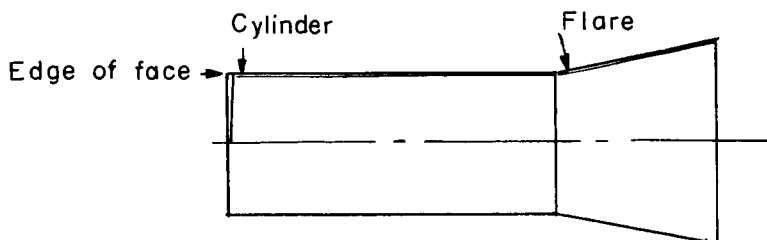


Figure 6.- Skin temperatures for impact Mach number of 0.5.

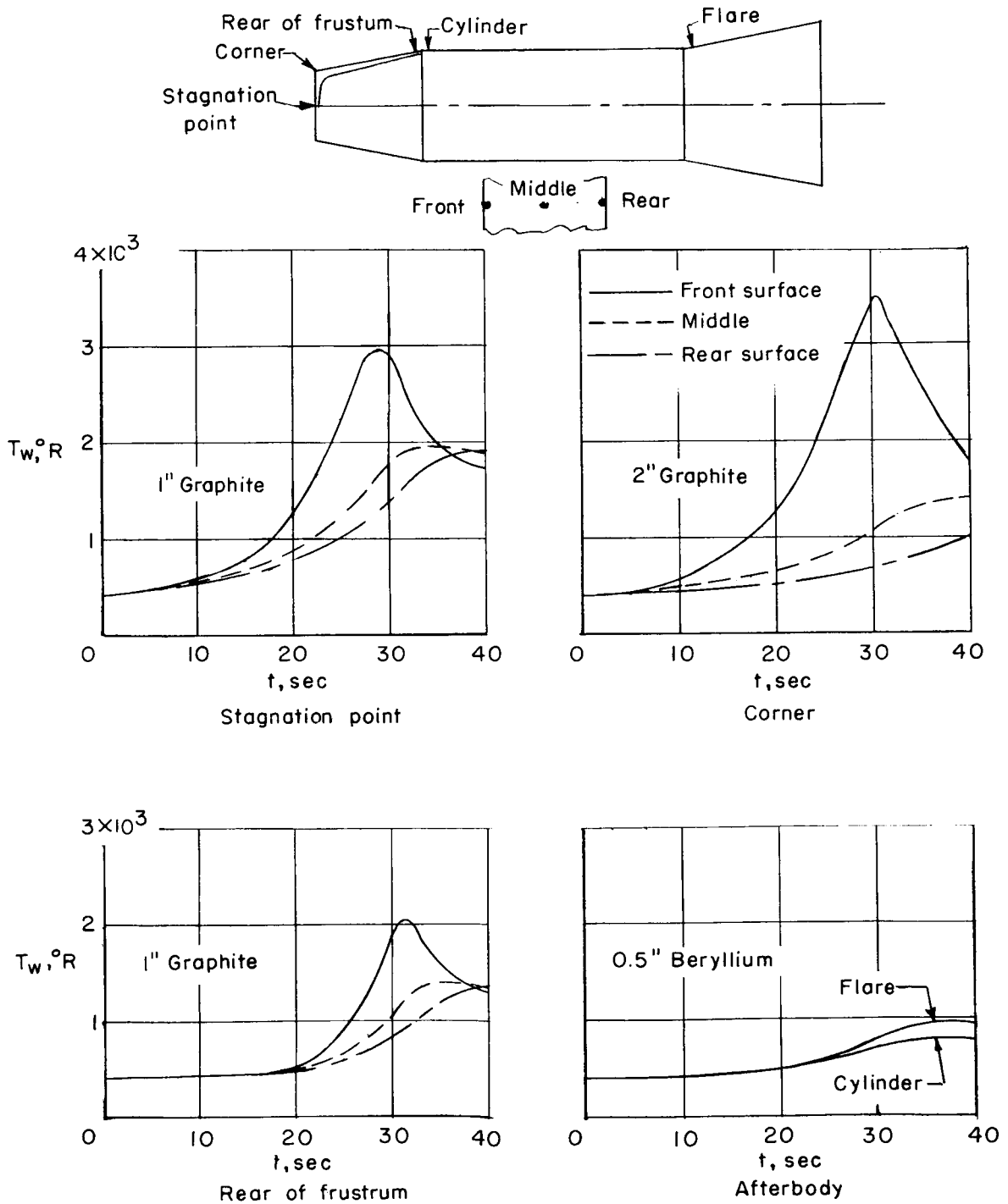


Figure 7.- Skin temperatures for impact Mach number of 1.05.

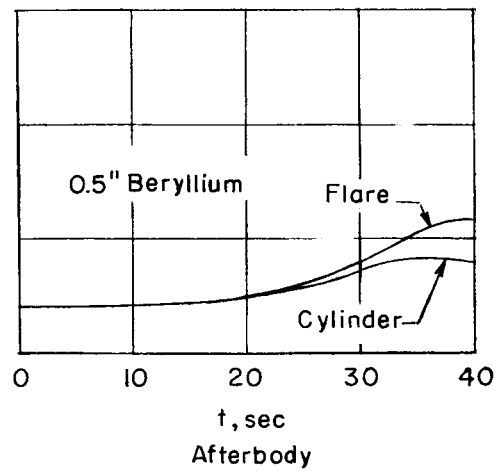
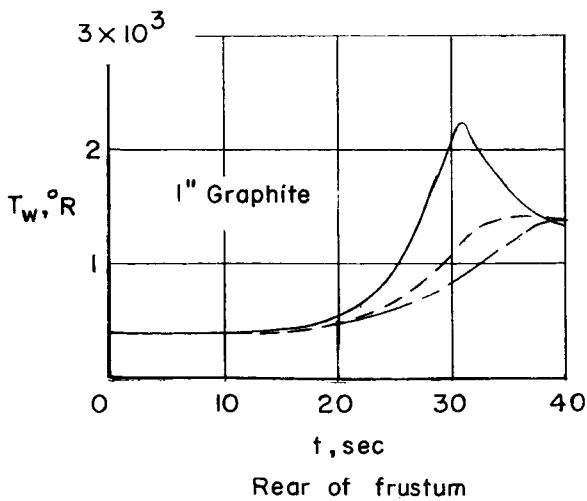
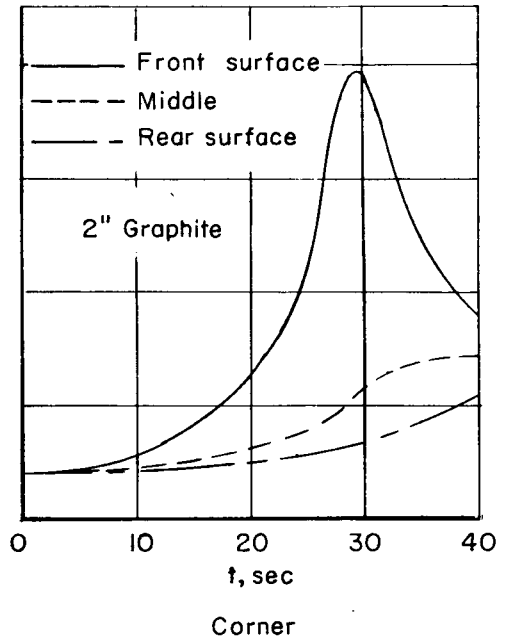
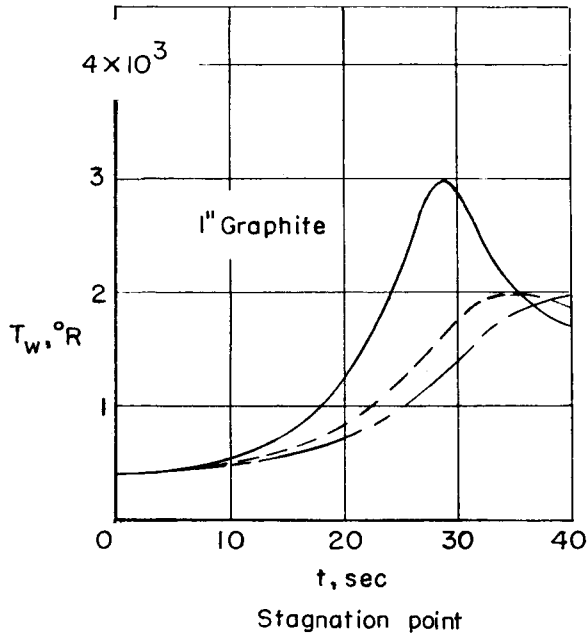
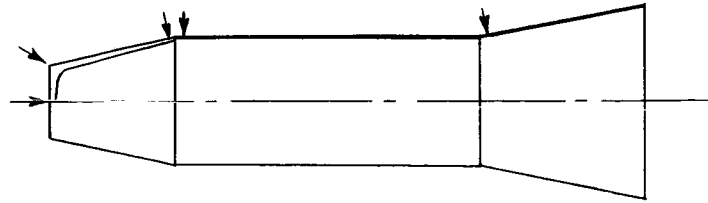


Figure 8.- Skin temperatures for impact Mach number of 1.49.

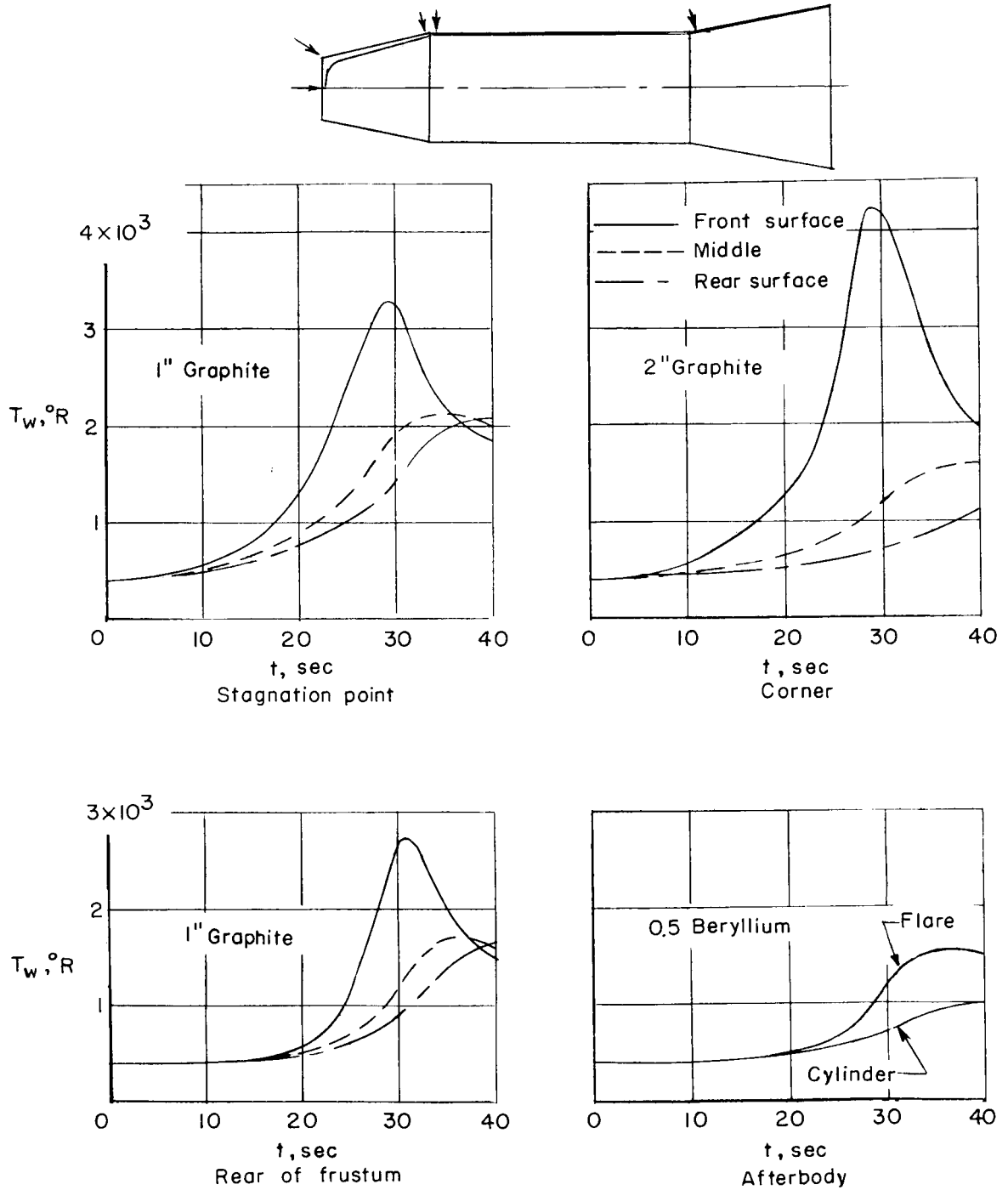


Figure 9.- Skin temperatures for impact Mach number of 1.89.



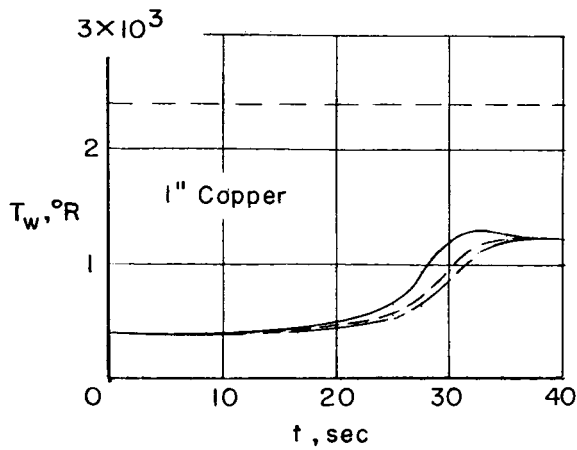
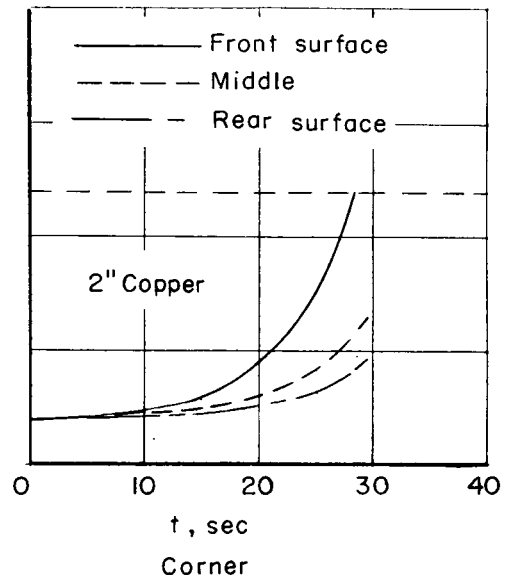
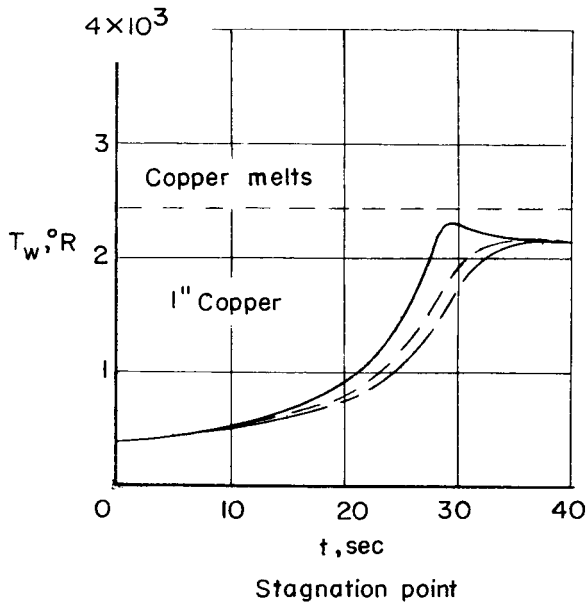
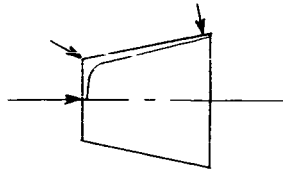


Figure 10.- Copper-nose temperature at impact Mach number of 1.05.